A chalcogen-bonded complex $(CH_3)_3N\cdots S{=}C{=}O$ characterised by rotational spectroscopy

Eva Gougoula[a], Joe A. Moxon[a] , Nicholas R. Walker[a,*] and Anthony C. Legon[b,*]

[a] Chemistry-School of Natural and Environmental Sciences, Newcastle University, Bedson Building, Newcastle-upon-Tyne NE1 7RU, UK.

[b]School of Chemistry, University of Bristol, Cantock's Close, Bristol BS8 1TS, UK.

Abstract

Rotational spectra of 5 isotopologues of $(CH_3)_3N\cdots S{=}C{=}O$ were observed by chirped-pulse, Fourier-transform microwave spectroscopy. Spectroscopic constants B_0, D_J, D_{JK} and the ^{14}N nitrogen nuclear quadrupole coupling constant $\chi_{aa}(^{14}N)$ determined for the symmetric-top isotopologues $(CH_3)_3N\cdots S{=}C{=}O$, $(CH_3)_3N\cdots{}^{34}S{=}C{=}O$, $(CH_3)_3N\cdots S{=}{}^{13}C{=}O$, $(CD_3)_3N\cdots S{=}C{=}O$ and $^{12}CH_3)_2(^{13}CH_3)^{14}N\cdots SCO$ show that the intermolecular binding involves a chalcogen bond to S rather than O. Changes in various properties (the distance r(N···S) and the force constants k_σ and $k_{\theta\theta}$ associated with intermolecular stretching and angular oscillation θ of the trimethylamine subunit, respectively) from those of $H_3N\cdots S{=}C{=}O$ allow of the effect of complete methylation of NH_3 on the chalcogen bond to be assessed.

*Corresponding authors.

Email addresses: Nick.Walker@newcatle.ac.uk (N. R. Walker). a.c.legon@bristol.ac.uk (A. C. Legon)

1. Introduction.

There has been much research activity recently concerned with non-covalent interactions. This has led IUPAC to make definitions of the hydrogen bond [1] in 2011, the halogen bond [2] in 2013 and the chalcogen bond this year [3]. The last of these was defined as follows: *A chalcogen bond (symbol ChB) involves a net attractive interaction between an electrophilic region associated with a chalcogen atom in a molecular entity and a nucleophilic region in another, or the same, molecular entity*. This definition applies to all phases but here we shall be concerned only with the interaction of pairs of molecules in isolation in the gas phase.

Although the chalcogen bond was named only in 2009 [4], isolated chalcogen-bonded, binary complexes were characterised, but not so-named, in the gas phase many years ago. For example, the complex HCN···SO_2 [5] is formed by the interaction of the electrophilic region near to the chalcogen atom S with the nucleophilic region of HCN, namely the axially-symmetric, non-bonding electron pair, to give a geometry in which HCN is perpendicular to the plane of the SO_2 nuclei. Similarly, the π electrons of ethene act as the nucleophilic site when the complex C_2H_4···SO_2 is formed [6]. Carbon disulphide forms weak chalcogen bonds in which H_2O [7] or NH_3[8] act as the electron donor and the region just outside the S atom on the $C_{\infty v}$ axis of CS_2 is the (weak) electrophile. Carbonyl sulphide is a congener of carbon disulphide in which one S atom is replaced by O, another chalcogen atom. A question of interest concerns which of the chalcogen atoms acts as the electrophile in forming

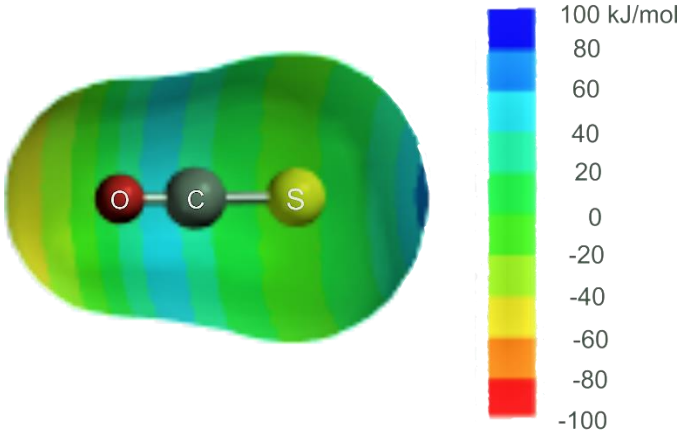

Figure 1. Molecular electrostatic surface potential (MESP) of OCS at the 0.001 bohr/Å^3 isosurface calculated at the MP2/6-311++G** level of theory by using the SPARTAN software. The front surface has been cut away to reveal the ball and stick model of OCS.

complexes with Lewis bases. Figure 1 shows the molecular electrostatic surface potential at the 0.001 bohr/Å^3 iso-surface of OCS as calculated at the MP2/6-311++G** level [9,10] of theory using the SPARTAN program [11]. There is clearly a positive potential energy region (blue) on the molecular axis near to S, which is electrophilic, while the other chalcogen atom O possesses a corresponding negative (orange) nucleophilic region near O. According to this diagram, the S atom should form a chalcogen bond with a Lewis base such as trimethylamine by interacting with the axial, non-bonding electron pair carried by N to give a symmetric-top complex $(CH_3)_3N\cdots S{=}C{=}O$. In this article, we report the detection and characterisation of such a chalcogen-bonded complex by means of its rotational spectrum. Analysis of the ground-state spectra of five isotopologues leads a variety of spectroscopic constants that can be interpreted to give details of the geometry, the strength of the chalcogen bond and the subunit dynamics. A novel type of chalcogen-bonded species involving the interaction of sulfur dioxide with dimethyl sulfide has been thoroughly investigated recently by microwave spectroscopy and quantum chemical calculations [12].

2. Experimental and theoretical methods

The ground-state rotational spectrum of a 1:1 chalcogen-bonded complex formed between carbonyl sulphide and trimethylamine was recorded in the 7.0-18.5 GHz region using the Chirped Pulse Fourier Transform Microwave (CP-FTMW) spectrometer at Newcastle University. The spectrometer operates in the 2.0-18.5 GHz frequency range and has been described in detail elsewhere [13].

Gaseous carbonyl sulphide (OCS, Sigma-Aldrich, ≥97.5%) and trimethylamine were mixed in equal quantities (~2%) and diluted (~98 %) in a buffer of argon gas (Ar, BOC PureShield 99.99%) at 6 bar constant pressure. The mixture was pulsed through a solenoid valve (Parker-Hannifin Series 9) and subsequently expanded into the high vacuum of the evacuated chamber of the spectrometer to form binary complexes $(CH_3)_3N\cdots SCO$ at an effective temperature of ~2 K. Generation of the fully deuterated species $(CD_3)_3N\cdots SCO$ was achieved by replacing trimethylamine by a sample of trimethylamine-d9. Eight sequential microwave pulses, each of 1 μs duration, were broadcast in a direction perpendicular to that of the direction of propagation of the expanding gas pulses, with each microwave pulse separately polarising molecular transitions after a delay long enough to allow decay of the preceding polarisation. Then the emission of radiation by molecules at rotational transition frequencies following each microwave pulse was collected in the form of a free induction decay (FID) by a 100 GS/s oscilloscope (Tektronix DPO72304SX). Using the oscilloscope's fast frame mode, an

FID was recorded for 20 μs after each polarisation. The FID's were coherently averaged in the time domain and Fourier transformed (FT) to the frequency domain spectrum using a Kaiser-Bessel window function. Various components of the microwave circuitry, including the oscilloscope, are phased-locked to a rubidium clock which provides a 10 MHz reference signal to ensure phase coherence in the time domain. Spectral linewidths of approximately 100 kHz at full width half maximum (FWHM) were achieved and transitions were measured with an estimated accuracy of about 10 kHz standard deviation (i.e. ~10% of the linewidth).

Geometry optimisations and frequency calculations for $(CH_3)_3N\cdots SCO$ were conducted at the MP2/aug-cc-pVTZ level [9,14, 15] of theory with the GAUSSIAN electronic structure package [16] and are available at files G1 and G2 in the Supplementary Material. The MESP of carbonyl sulphide was calculated at the MP2/6-311++G** level [9,10] with the aid of the SPARTAN program [11].

3. Results

3.1 Spectral analysis

The ground-state rotational spectra of the five isotopologues $(^{12}CH_3)_3{}^{14}N\cdots{}^{32}S^{12}C^{16}O$, $(^{12}CH_3)_3{}^{14}N\cdots{}^{34}S^{12}C^{16}O$, $(CH_3)_3N\cdots{}^{32}S^{13}C^{16}O$, $(^{12}CH_3)_2(^{13}CH_3)^{14}N\cdots{}^{32}S^{12}C^{16}O$ and $(CD_3)_3{}^{14}N\cdots{}^{32}S^{12}C^{16}O$ were recorded, the first four in their natural abundances of about 92, 4.2, 1.1 and 3.3 %, respectively, by using isotopically normal samples of trimethylamine and carbon disulphide, while that of $(CD_3)^{14}N\cdots{}^{32}S^{12}C^{16}O$ was obtained with the aid of an isotopically enriched sample of trimethylamine-d9. Observed frequencies were fitted in an iterative, least-squares analysis using Western's PGOPHER program [17]. The final cycle of the fit for each isotopologue is included in the Supplementary Material as Tables S1 to S5. The determined spectroscopic constants are given in Table 1. Quantum chemical calculations at the MP2/aug-cc-pVTZ level give the equilibrium values of B, D_J, and the coupling constant $\chi_{aa}(^{14}N)$ in satisfactory agreement with zero-point values determined experimentally, as may be seen from the Supplementary Material, Gaussian files G1 and G2. No imaginary frequencies were found for $(CH_3)_3N\cdots SCO$. The spectra of observed isotopologues, except the singly substituted ^{13}C species, were of the prolate symmetric-top type. The Hamiltonian chosen to fit the symmetric-top spectra had the form

$$H = H_R - {}^1/_6\,\mathbf{Q}(^{14}N):\nabla\mathbf{E}(^{14}N) \qquad (1),$$

where H_R is the familiar Hamiltonian for a semi-rigid, symmetric-rotor molecule in its vibrational ground state [18] and the second term is the energy operator describing the interaction of the ^{14}N nuclear electric quadrupole moment $\mathbf{Q}(^{14}N)$ with the electric field gradient $\nabla\mathbf{E}(^{14}N)$ at the nitrogen nucleus. The matrix of H was constructed in the $\boldsymbol{I}_N + \boldsymbol{J} = \boldsymbol{F}$ coupled basis and diagonalized in blocks of F. For a prolate, symmetric-top molecule carrying a ^{14}N nucleus on its symmetry axis a, the coupling tensor is diagonal and only the single independent component $\chi_{aa}(^{14}N) = eQ(^{14}N)\,\partial^2V(^{14}N)/\partial a^2$ of the tensor is necessary to describe the hyperfine structure. The resolved hyperfine structure on three K components of the J =6 →5 transition is shown in Figure 2.

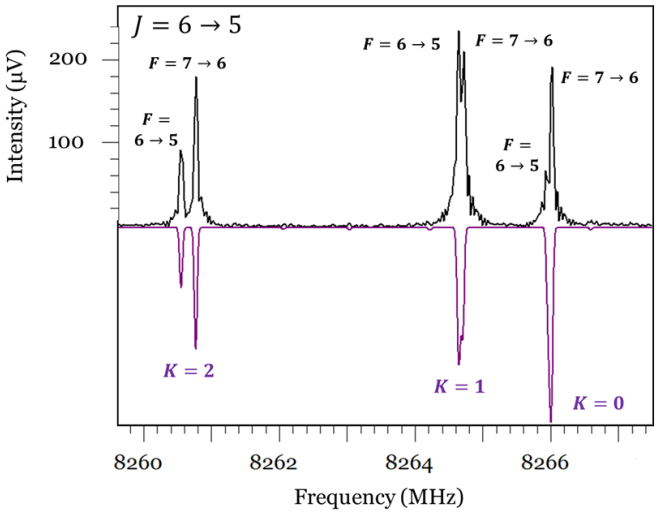

Figure 2. A recording of K components (K = 0, 1 and 2) of the J = 6 →5 transition of $(^{12}CH_3)_3{}^{14}N\cdots{}^{32}S{}^{12}C{}^{16}O$. Some ^{14}N nuclear quadrupole hyperfine components are resolved for K = 1 and 2, while the K= 0 transition shows only incipient resolution. The downward pointing transitions are those simulated with the spectroscopic constants given in Table 1.

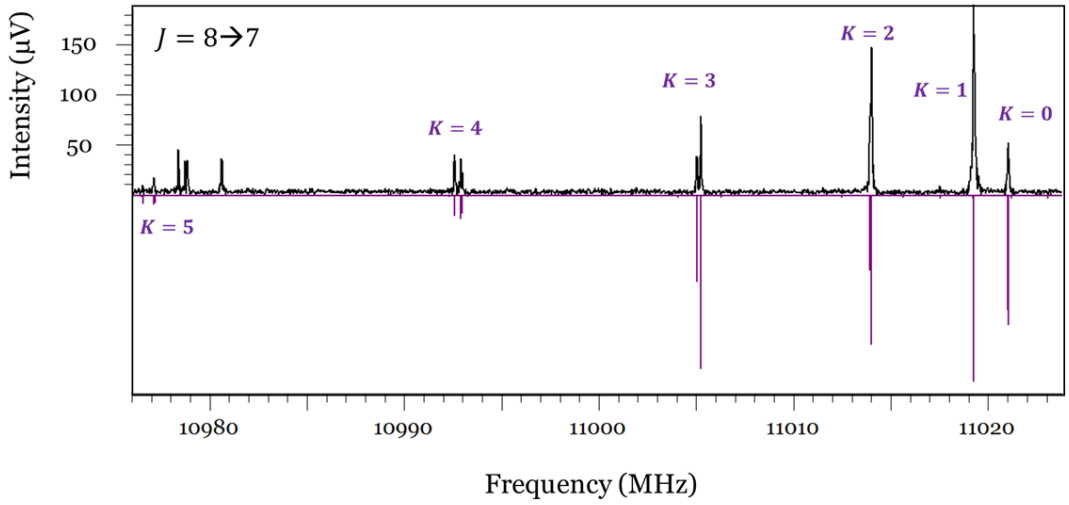

Figure 3. A recording of the $J = 8 \rightarrow 7$ transition of $(^{12}CH_3)_3{}^{14}N\cdots{}^{32}S{}^{12}C{}^{16}O$ showing the dependence on K^2 and the fact that the ^{14}N nuclear quadrupole hyperfine structure begins to be resolved only at higher K in this high J transition. The downward pointing spectrum is a simulation based on the spectroscopic constants from Table 1.

The fact that transitions with J quantum numbers as high as 13 were observed meant that the ^{14}N-nuclear quadrupole hyperfine structure of some transitions was not resolved and in those cases it was assumed that the measured frequency corresponded to that of the $F+1 \rightarrow F$ component of largest F. This can be seen clearly in Figure 3, which displays several K components of the $J = 8 \rightarrow 7$ transition for the most abundant isotopologue. The hyperfine structure is unresolved for the K = 0 and 1 transitions but begins to be resolved for higher K. For $(CD_3)^{14}N\cdots{}^{32}S{}^{12}C{}^{16}O$, the additional (unresolved) quadrupole coupling arising from the presence of 9 D (I =1) nuclei led to line broadening and precluded the resolution of the ^{14}N hyperfine structure.

The observation of some quite high J transitions also made it necessary to examine the effects of including sextic centrifugal distortion terms in the semi-rigid rotor Hamiltonian in addition to the usual quartic terms involving the constants D_J and D_{JK}. The distortion constant H_{JK} was just determinable, as may be seen from the set of spectroscopic constants recorded in Table 1, but the remaining sextic constants did not contribute significantly and were therefore not released.

The spectrum of the isotopologue $(^{12}CH_3)_2\,(^{13}CH_3)^{14}N\cdots{}^{32}S={}^{12}C={}^{16}O$ was that of a nearly-prolate asymmetric rotor in which it was possible to identify only *a*-type, R-branch transitions of the type $(J+1)_{n,J+1} \rightarrow J_{n,J}$ and $(J+1)_{n,J} \rightarrow J_{n,J-1}$, for n =0,1,2 and 3. Frequencies of these transitions were fitted to give the rotational constants $B_0 + C_0$, $B_0 - C_0$ and the centrifugal distortion constants Δ_J, Δ_{JK} and H_{JK} appropriate to a nearly prolate asymmetric rotor [18]. Nuclear quadrupole coupling was not well resolved in the observed transitions and therefore $\chi_{aa}(^{14}N)$ was set to the value determined for the parent species. The same procedure was adopted for $\chi_{aa}(^{14}N)$ of the isotopologue $(CH_3)_3{}^{14}N\cdots{}^{32}S={}^{13}C={}^{16}O$

3.2 Molecular properties determined from spectroscopic constants.

3.2.1 Geometry.

Only zero-point spectroscopic constants were obtained from the rotational spectra of the various isotopologues of $(CH_3)_3N\cdots SCO$. The rotational constants can be interpreted to provide a r_0 value of the N to S distance and the centrifugal distortion constant D_J and D_{JK} can be used to obtain

two force constants associated with the low-frequency intermolecular motion of the complex, namely the intermolecular stretching force constant k_σ, and the force constant $k_{\theta\theta}$ associated with intermolecular bending at N.

The fact that the parent isotopologue, the species with either ^{34}S- or ^{13}C in the OCS subunit, and D_9- substituted species are symmetric-top molecules shows that the OCS subunit lies on the symmetry axis. Moreover, the changes in B_0 on ^{34}S and on ^{13}C substitution in the parent isotopologue lead to the r_s coordinates [19] of sulfur and carbon in the principal inertia axis system of $^{16}O^{12}C\ ^{32}S$ $a_S = (\Delta I_b/\mu_s)^{\frac{1}{2}} =$ 1.1730 (13) Å and 2.7367(6) Å, respectively, where ΔI_b is the change in the principal moment of inertia of the parent molecule that accompanies the isotopic substitution and μ_s is the reduced mass of the substitution. The errors were calculated by the method in ref.[19]. Such errors merely reflect experimental error in rotational constants and the likely to be underestimates as a result of the floppiness of the complex. The r_s coordinates are of interest only because they confirm that the sulphur atom lies closer to the centre of mass of the complex than does C and therefore (given the posithtion of ^{14}N established below) that the order of the axial atoms is N···S=C=O. The position of ^{14}N as adjacent to S is indicated by the change in the moment of inertia of the complex accompanying complete deuteration of the trimethylamine subunit. This change is consistent only with the D atoms lying further from the complex centre of mass than ^{14}N. Hence, the S atom is involved a halogen-bond interaction with the non-bonding electron pair of N.

In weakly bound complexes, the largest contribution to the main difference between zero-point and equilibrium rotational constants probably results from the contributions of the intermolecular bending modes. A model of the complex that removes such contributions was proposed by Klemperer and co-workers [20] and can be understood with the aid of Figure 4.

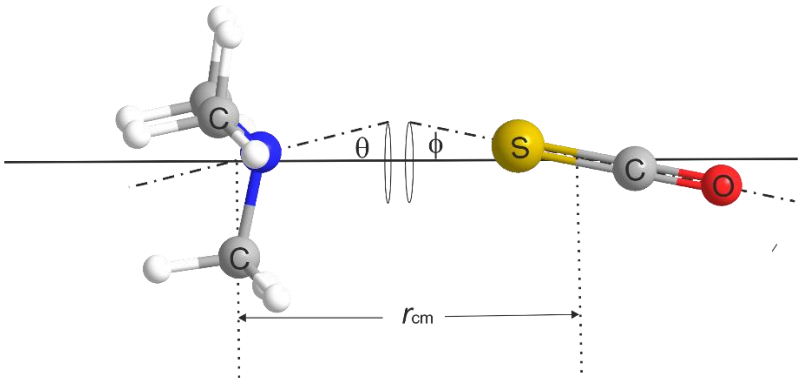

Figure 4. Schematic diagram of the model used to determine the distance r_{cm} between the centres of mass of the $(CH_3)_3N$ and SCO subunits of the $(CH_3)_3N\cdots SCO$ complex from the observed zero-point rotational constants by allowing for the angular oscillations θ and ϕ.

The subunits $(CH_3)_3N$ and SCO are each assumed to undergo two-dimensionally-isotropic, angular oscillations about their mass centres described by the angles θ and ϕ, respectively, indicated in Figure 4. The distance r_{cm} between the mass centres is assumed fixed, which means that the contribution of the intermolecular stretching mode is neglected. θ and ϕ are the angles made by the C_3 symmetry axis of $(CH_3)_3N$ and the internuclear axis of S=C=O, respectively, with the line r_{cm}. It can be demonstrated that the zero-point moment of inertia I_b^0 of the complex is related to the ground-state moments of inertia $I_b^{(CH_3)_3N}$ and I_b^{SCO} of the component molecules in reasonable approximation by [20]

$$I_b^0 \approx \mu r_{cm}^2 + \tfrac{1}{2} I_b^{(CH_3)_3N} \langle 1 + \cos^2\theta \rangle + \tfrac{1}{2} I_b^{(CH_3)_3N} \langle \sin^2\theta \rangle + \tfrac{1}{2} I_b^{SCO} \langle 1 + \cos^2\phi \rangle \qquad (2),$$

in which c is the symmetry axis of the free $(CH_3)_3N$ molecule. It is possible to obtain operationally defined averages of the angle θ from two sources. First, if the perturbation of the electric field gradient at ^{14}N by the presence nearby of S=C=O can be ignored, the ^{14}N nuclear quadrupole coupling constant $\chi_{aa}(^{14}N)$ of the complex in the zero-point state is related to that $\chi_0(^{14}N)$ of the free molecule $(CH_3)_3{}^{14}N$ according to

$$\chi_{aa}\left(^{14}N\right) = \frac{1}{2}\chi_0(^{14}N)\langle 3\cos^2\theta - 1\rangle_{0,0} \qquad (3),$$

where the angular brackets denote the zero-point average. Then, the operational definition of θ_{av} is

$$\theta_{av} = \cos^{-1}\langle\cos^2\theta\rangle_{0,0}^{\frac{1}{2}} = \cos^{-1}\left(\frac{2\chi_{aa}(^{14}N)}{3\chi_0(^{14}N)} + \frac{1}{3}\right)^{\frac{1}{2}} \qquad (4).$$

By using the value of $\chi_0(^{14}N)$ of $(CH_3)_3{}^{14}N$ [21] from Table 2 and that $\chi_{aa}\left(^{14}N\right)$ of the parent isotopologue $(^{12}CH_3)_3{}^{14}N\cdots{}^{32}S{}^{12}C{}^{16}O$ from Table 1, the result is θ_{av} = 12.0(6) º. It will be shown below that it is possible to obtain the quantity $\langle\theta^2\rangle_{0,0}$ from the centrifugal distortion constants D_J and D_{JK}. For the parent isotopologue, the result is $\langle\theta^2\rangle_{0,0}{}^{1/2}$ = 12.7 º, in excellent agreement with that from eq.(4). Estimating a value of the amplitude of the SCO subunit motion ϕ_{av} is less straight forward. This would be possible by using $\chi_{aa}(^{33}S)$ for the ^{33}S isotopologue of the complex but the spectrum of $(^{12}CH_3)_3{}^{14}N\cdots{}^{33}S{}^{12}C{}^{16}O$ was too weak to observe. However, recent work on the related chalcogen-bonded system $H_3N\cdots S=C=S$ [8], shows that it is about a factor of 2 more weakly bound than $(CH_3)_3N\cdots S=C=O$, according to one criterion of binding strength, namely the intermolecular

stretching force constants k_σ = 3.9 [8] and 7.6 N m^{-1} (see Section 3.2.2) , respectively. Likewise, *ab initio* calculations at the MP2/aug-cc-pVTZ level yield the BSSE-corrected dissociation energies D_e = 7.7 kJ mol^{-1} and 14.2 kJ mol^{-1}, respectively, to confirm the factor of 2 in the binding strength. It was established in ref. [8] that ϕ_{av} = 10º for $H_3N\cdots S{=}C{=}S$. Given the greater strength of $(CH_3)_3N\cdots SCO$, it is reasonable to assume that ϕ_{av} for this complex is 7(3)º. Assumed values in the range of ±3º then includes the $H_3N\cdots S{=}C{=}S$ value as an upper limit. Angles in the range 4 to 7º lead to negligible change in the geometrical conclusions presented here. The agreement between the two methods of estimating θ_{av} suggests the range ±1º for this angle. The values of r_{cm} and $r(N\cdots S) = r_{cm} - r - r'$, where r and r' ar e the distances of N and S from the centres of mass of the separate molecules $(CH_3)_3N$ and SCO, respectively, and were obtained from spectroscopic constants of the separate molecules, which are given in Table 2 and are taken from refs. [22] and [23]. The results obtained under these assumptions are recorded in Table 3. The errors are those that arise from assumed errors of 1º and 3º in θ_{av} and ϕ_{av}, respectively, and are relatively small because it happens that the distances are not strongly dependent on these angles. There is good agreement among the $r(N\cdots S)$ values of the four symmetric-top isotopologues. The same approach cannot be applied to $(^{12}CH_3)_2(^{13}CH_3)^{14}N\cdots{}^{32}S{=}{}^{12}C{=}{}^{16}O$ because it is an asymmetric rotor.

3.2.2 Intermolecular quadratic force constants

Two quadratic force constants associated with the intermolecular modes of $(CH_3)_3N\cdots SCO$ can be determined from the centrifugal distortion constants D_J and D_{JK} of the complex. These are the intermolecular stretching constant k_σ and the angle bending constant $k_{\theta\theta}$.

In the approximation of rigid, unperturbed subunits, Millen [24] showed that, for a symmetric-top complex such as $(CH_3)_3N\cdots SCO$, k_σ is related to the constants D_J and B_0 in reasonable approximation by

$$k_\sigma = \left(16\pi^2\mu B_0^3/D_J\right)\left\{1 - \left(B_0/B^{(CH_3)_3N}\right) - \left(B_0/B^{OCS}\right)\right\} \qquad (5),$$

although strictly the constants should all be equilibrium values. In the absence of equilibrium constants, zero-point quantities have been used. Values of k_σ obtained for the four symmetric-top isotopologues of $(CH_3)_3N\cdots SCO$ via eq.(5) are included in Table 3. The necessary rotational constants of trimethylamine [21] and carbonyl sulphide [23] are reported in Table 2. The internal consistency of the values is satisfactory. The errors quoted arise from the errors in the D_J values and do not account for unknown errors arising from use of zero-point constants in place of equilibrium values.

When the model of the angular motion of the $(CH_3)_3N$ subunit defined in Section 3.2.1 with the aid of Figure 4 is assumed and this subunit is again described as a two-dimensional isotropic harmonic oscillator, it can be shown [25] that the angle bending force constant $k_{\theta\theta}$ is related to the linear combination of centrifugal distortion constants $D = 2D_J + D_{JK}$ by the equation

$$k_{\theta\theta} = (2h/D)B_0^2\left[B_0/B^{(CH_3)_3N} - 1\right] \qquad (6),$$

in which the spectroscopic constants involved should also be equilibrium values. The values of $k_{\theta\theta}$ obtained when zero-point constants (available from Tables 1 and 2) are used in eq.(6) are included in Table 3. There is excellent internal consistency among the values for the four symmetric-top isotopologues.

It was shown in ref. [25] that the average of the square of the bending angle $\langle\theta^2\rangle_{0,0}$ in the zero-point state is related to $k_{\theta\theta}$via eq.(7):

$$\langle\theta^2\rangle_{0,0} = (h/2\pi)\left(k_{\theta\theta}I_b^{(CH_3)_3N}\right)^{-1/2} \qquad (7)$$

Values of $\theta_{\mathrm{av}} = \langle\theta^2\rangle^{\frac{1}{2}}$ so determined are included in Table 3. The errors in $k_{\theta\theta}$ and θ_{av} arising from errors in the spectroscopic constants involved in eqs.(6) and (7) are negligible. Presumably larger, but unknown, errors result from the use of zero-point instead of equilibrium values in eqs.(6) and (7).

4. Discussion and conclusions.

An investigation of a complex formed by trimethylamine and carbonyl sulphide in the gas phase by means of its rotational spectrum has concluded that the parent isotopologue

$(^{12}CH_3)_3{}^{14}N\cdots{}^{32}S^{12}C^{16}O$ is a symmetric-top molecule with the atoms in the indicated order, as confirmed by means of the ^{34}S and ^{13}C species associated with the SCO subunit (observed in natural abundance) and the $(CD_3)_3{}^{14}N$ species, all of which are symmetric-top complexes. The weak intermolecular binding is therefore via a chalcogen bond formed by S of OCS (rather than O) with the non-bonding electron pair of trimethylamine, which lies along the its C_3 axis. This observation is consistent with the MESP of carbonyl sulphide shown in Figure 1, from which it is concluded that a point near to S on the molecular axis is the most electrophilic region of the molecule.

Interpretation of the spectroscopic constants based on unperturbed monomer geometries leads to the following properties of the complex: the intermolecular distance r(N···S), the intermolecular stretching force constant k_σ and the angle bending force constant $k_{\theta\theta}$ associated with bending of the trimethylamine subunit, as well as the operationally defined angles $\theta_{\mathrm{av}} = \cos^{-1}\langle\cos^2\theta\rangle^{\frac{1}{2}}$ determined from the ^{14}N nuclear quadrupole coupling constant and $\langle\theta^2\rangle^{1/2}$ determined from the force constant $k_{\theta\theta}$ obtained by use of eq.(6). The values of these properties for the parent isotopologue of $(CH_3)_3N\cdots SCO$ are compared in Table 4 with those of the related complexes $H_3{}^{14}N\cdots{}^{32}S^{12}C^{16}O$ [26] and $H_3N\cdots{}^{32}S^{12}C^{32}S$ [8], in both of which the non-covalent interaction is also via a chalcogen bond formed by S with the axial, non-bonding electron pair carried by N. A value of r_e(N···S) =3.032 Å for $(CH_3)_3N\cdots S{=}C{=}O$ was also determined by means of a geometry optimisation at the MP2/aug-cc-pVTZ level of theory. This is 0.03 Å shorter than the value quoted in Table 4, as expected. Although the value in Table 4 is corrected to some extent for the large amplitude angular oscillations in the zero-point state through eq.(2), the intermolecular stretching mode is ignored. This mode is likely to be responsible for most of the lengthening in the zero-point state.

Table 4 shows that, according to the criteria listed there, the complex $(CH_3)_3N\cdots SCO$ is more strongly bound than either $H_3N\cdots SCO$ or $H_3N\cdots SCS$. This conclusion is consistent with the generally held view that methylation of ammonia leads to an increase in the nucleophilicity of the non-bonding electron pair. Table 4 also demonstrates that $H_3N\cdots SCO$ and $H_3N\cdots SCS$ are very similar according to the properties r(N···S) and $k_{\theta\theta}$, that is the chalcogen-bonding interaction is not significantly changed whether the electrophile region is S of S=C=O or S=C=S. Finally, we note from Table 4 that the

operationally defined oscillation angles of the ammonia and trimethylamine subunits θ_{av} determined from ^{14}N nuclear quadrupole coupling constants using eq.(4) are systematically lower that those $\langle\theta^2\rangle^{1/2}$ obtained from $k_{\theta\theta}$ and eq.(7). This probably arises in part by the reduction in the magnitude of $\chi_{aa}(^{14}N)$ because of the electric field gradient at N due to the presence nearby of the SCS or SCO subunits.

5. Acknowledgements

The authors thank Newcastle University for a research studentship (for E.G.) and the European Research Council for project funding (Grant No. CPFTMW-307000). ACL thanks the University of Bristol for A Senior Research Fellowship.

6. References

[1] E. Arunan, G. R. Desiraju, R. A. Klein, J. Sadlej, S. Scheiner, I. Alkorta, D. C. Clary, R. H. Crabtree, J. J. Dannenberg, P. Hobza, H. G. Kjaergaard, A. C. Legon, B. Mennucci, and D. J. Nesbitt, *Pure and Appl. Chem.*, 83 (2011) 1637-1641.

[2] G. R. Desiraju, P. S. Ho, L. Kloo, A. C. Legon, R. Marquardt, P. Metrangolo, P. A. Politzer, G. Resnati and K. Rissanen, Pure and Appl. Chem. 85 (2013) 1711-1713.

[3] C. B. Aakeroy, D. L. Bryce, G. R. Desiraju, A. Frontera, A. C. Legon, F. Nicotra, K. Rissanen, S. Scheiner, G. Terraneo, P. Metrangolo and G. Resnati, *Pure Appl. Chem.* …..(2019).

[4] W. Wang, W. B. Ji, and Y. Zhang, J. Phys. Chem. A 113 (2009) 8132–8135.

[5] E. J. Goodwin and A. C. Legon, J. Chem. Phys. 85 (1986) 6828-36.

[6] A. M. Andrews, A. Taleb-Bendiab, M. S. LaBarge, K. W. Hillig and R. L. Kuczkowski, J. Chem. Phys., 93 (1993) 7030–7040.

[7] T. Ogata and F. J. Lovas, J Mol. Spectrosc. 162 (1993) 505-512.

[8] E. Gougoula, C. Medcraft, I. Alkorta, N. R. Walker and A. C. Legon, J. Chem. Phys. 150 (2019) 084307.

[9] C. Möller and M. S. Plesset, Phys. Rev. 46 (1934) 618-622.

[10] M. M Francl, W. J. Pietro, W.J. Hehre, J. S. Binkley, M. S. Gordon, D. J. DeFrees, and J. A. Pople, J. Chem. Phys.77 (1982) 3654-3665.

[11] B. J. Deppmeier, A. J. Driessen, T. S. Hehre, W. J. Hehre, J. A. Johnson, P. E.Klunzinger, J. M. Leonard, I. N. Pham, W. J. Pietro, J. Yu, Y. Shao, L. Fusti-Molnar, Y. Jung, J. Kussmann,

C. Ochsenfeld, S. T. Brown, A. T. B. Gilbert, L. V. Slipchenko, S. V. Levchenko, D. P. O'Neill, R. A. Di Stasio, Jr., R. C. Lochan, T. Wang, G. J. O. Beran, N. A. Besley, J. M. Herbert, C. Y. Lin, T. Van Voorhis, S. H. Chien, A. Sodt, R. P. Steele, V. A. Rassolov, P. E.Maslen, P. P. Korambath, R. D. Adamson, B. Austin, J. Baker, E. F. C. Byrd, H. Dachsel, R. J. Doerksen, A. Dreuw, B. D. Dunietz, A. D. Dutoi, T. R. Furlani, S. R. Gwaltney, A. Heyden, S. Hirata, C.-P. Hsu, G. Kedziora, R. Z. Khalliulin, P. Klunzinger, A. M. Lee, M. S. Lee, W. Liang, I. Lotan, N. Nair, B. Peters, E. I. Proynov, P. A. Pieniazek, Y. M. Rhee, J. Ritchie, E. Rosta, C. D. Sherrill,A. C. Simmonett, J. E. Subotnik, H. L. Woodcock III, W. Zhang, A. T. Bell,A. K. Chakraborty, D. M. Chipman, F. J. Keil, A. Warshel, W. J. Hehre, H.F. Schaefer III, J. Kong, A. I. Krylov, P. M. W. Gill, and M. Head-Gordon. SPARTAN'14 Mechanics Program: (Win/64b) Release 1.1.8, Wavefunction,Inc., SPARTAN, Inc., 2014.

[12] D. A. Obenchain, L. Spada, S. Alessandrini, S. Rampino, S. Herbers,N. Tasinato, M. Mendolicchio, P. Kraus, J. Gauss, C. Puzzarini, J.-U. Grabow, and V. Barone, Angew. Chem. Int. Ed. 57, (2018) 15822 –15826.

[13] D. P. Zaleski, S. L. Stephens, and N. R. Walker, Phys. Chem. Chem. Phys. 16 (2014) 25221–25228.

[14] R.A. Kendall, T.H. Dunning, Jr. and R.J. Harrison, J. Chem. Phys. 96 (1992) 6796.

[15] D.E. Woon and T.H. Dunning, Jr. J. Chem. Phys. 98 (1993) 1358.

[16] M. J. Frisch, G. W. Trucks, H. B. Schlegel, G. E. Scuseria, M. A. Robb, J. R. Cheeseman, G. Scalmani, V. Barone, B. Mennucci, G. A. Petersson, H. Nakatsuji, M. Caricato, X. Li, H. P. Hratchian, A. F. Izmaylov, J. Bloino, G. Zheng, J. L. Sonnenberg, M. Hada, M. Ehara, K. Toyota, R. Fukuda, J. Hasegawa, M. Ishida, T. Nakajima, Y. Honda, O. Kitao, H. Nakai, T. Vreven, J. A. Montgomery, Jr., J. E. Peralta, F. Ogliaro, M. Bearpark, J. J. Heyd, E. Brothers, K. N. Kudin, V. N. Staroverov, T. Keith, R. Kobayashi, J. Normand, K. Raghavachari, A. Rendell, J. C. Burant, S. S. Iyengar, J. Tomasi, M. Cossi, N. Rega, J. M. Millam, M. Klene, J. E. Knox, J. B. Cross, V. Bakken, C. Adamo, J. Jaramillo, R. Gomperts, R. E. Stratmann, O. Yazyev, A. J. Austin, R. Cammi, C. Pomelli, J. W. Ochterski, R. L. Martin, K. Morokuma, V. G. Zakrzewski, G.A. Voth, P. Salvador, J. J. Dannenberg, S. Dapprich, A. D. Daniels, O. Farkas, J. B. Foresman, J. V. Ortiz, J. Cioslowski, and D. J. Fox, GAUSSIAN 09, Revision D.01, Gaussian, Inc., Wallingford, CT, 2013.

[17] PGOPHER, a Program for Simulating Rotational Structure, Designed by C.M. Western, version 6.0.202, University of Bristol, 2010, available at http://pgopher.chm.bris.ac.uk. See als o: C. M. Western, J.Quant.Spectr.&Rad.Transfer, 186 (2017) 221–242.

[18] Microwave Molecular Spectra, W. Gordy and R. L. Cook, John Wiley & Sons, New York, 1984, Chapters 6 and 8.

[19] C. C. Costain, J. Chem. Phys. 29 (1958) 864-874.

[20] G. T. Fraser, K. R. Leopold, and W. Klemperer, J. Chem. Phys. 81 (1984) 2577–2584.

[21] X. L. Li, R. Bocquet, D. Petitprez, D . Boucher, L. Poteau and J. Demaison. J. Mol Spectrosc. 172 (1995) 449-445.

[22] J. E. Wollrab and V. W. Laurie, J. Chem. Phys. 51 (1969) 1580-1583.

[23] Triatomic Spectral Database, NIST Standard Reference Database 117. Frank J. Lovas, J. S. Coursey, S. A. Kotochigova, J. Chang, K. Olsen, and R. A. Dragoset. https://www.nist.gov/pml/triatomic-spectral-database

[24] D. J. Millen, Can. J. Chem. 63 (1985) 1477-1479.

[25] A.C. Legon and D.G. Lister, Chem. Phys. Lett. 238 (1995) 156-162. [Note that the version of eqn. (6) given in this reference has the factor of 2 in the denominator instead of the numerator].

[26] X.Liu and Y. Xu. Phys. Chem. Chem. Phys. 13 (2011) 14235-14242.

Tables.

Table 1. Spectroscopic constants of the vibrational ground state of $CH_3)_3N\cdots SCO$ isotopologues

Property	$(CH_3)_3N\cdots SCO$[a]	$(CH_3)_3N\cdots{}^{34}SCO$	$(CD_3)_3N\cdots SCO$	$(CH_3)_3N\cdots S^{13}CO$	$(CH_3)_2(^{13}CH_3)N\cdots SCO$
B_0/MHz	688.8526(3)[b]	686.3259(3)	627.7811(2)	681.9261(6)	682.9506(4)[c]
D_J/kHz	0.2707(10)	0.2726(15)	0.2223(8)	0.267(3)	0.276(2)
D_{JK}/kHz	110.38(3)	109.34(9)	124.28(3)	109.2(2)	110.5(1)
H_{JK}/Hz	1.2(1)	2.2(4)	2.1(1)	(1.2)[d]	0.93(5)
$\chi_{aa}(^{14}N)$/MHz	-5.141(35)	-5.33(19)	(-5.141)[d]	(-5.141)[d]	(-5.141)[d]
N[e]	63	29	49	13	24
σ_{rms}/kHZ[f]	8.0	8.6	8.3	12.8	9.7

[a] Absence of a mass number implies the most abundant nuclide

[b] Numbers in parentheses are one standard deviation in units of the last significant figure.

[c] This quantity is $(B_0+C_0)/2$. The constant(B_0-C_0) =1.8283(6) MHz was also determined in the fit of this asymmetric-top molecule (see text). The centrifugal distortion constants are also those appropriate to an asymmetric-top molecule (see text), namely Δ_J, Δ_{JK} and H_{JK}.

[d] These values were transferred from the parent isotopologue and held fixed in the fit.

[e] Number of hyperfine components included in the fit. [f] Root-mean-square deviation of the fit.

Table 2. Spectroscopic and molecular properties of isolated trimethylamine and carbonyl sulphide

Property	Trimethylamine		Carbonyl sulphide		
	$(CH_3)_3{}^{14}N$	$(CD_3)_3{}^{14}N$	$^{32}S^{12}C^{16}O$	$^{34}S^{12}C^{16}O$	$^{32}S^{13}C^{16}O$
3	8720.86[a]	6390.6789[b]	6081.49248(8)[c]	5932.838(5)[c]	6061.92510[c]
C_0/MHz	4984.5[d]	3767.45[d]	-	-	-
$\chi_0(^{14}N)$/MHz	-5.5002(18)[e]	-	-	-	-
r/Å	0.3598[f]	[d]0.3874	-	-	-
r'/Å[g]	-	-	1.0389	1.0054	1.0476

[a] Ref.[22]. [b] Determined in this work from measurement of the J =1→0 transition under the assumption D_J = 7.29 kHZ (from parent species reported in ref.[22])

[c] Ref.[23]. [d] Calculated from the r_s geometry reported in ref.[22].

[e] Ref.[21] [f] r_s coordinate of ^{14}N reported in ref.[22]. r is the distance of ^{14}N from the $(CH_3)_3N$ mass centre.

[g] Calculated from the geometry r_0(C=S) =1.5645(9) Å and r_0(C=O) = 1.0389(1) Å obtained by fitting the ground-state rotational constants of $^{32}S^{12}C^{16}O$, $^{34}S^{12}C^{16}O$, $^{32}S^{12}C^{18}O$ and $^{32}S^{13}C^{16}O$ given in ref.[23]. r' is the distance of S from the mass centre of the appropriate isotopologue of OCS.

Table 3. Properties of the complex $(CH_3)_3N\cdots SCO$ determined from its ground-state rotational spectrum.

Property	$(CH_3)_3N\cdots SCO$[a]	$(CH_3)_3N\cdots{}^{34}SCO$	$(CD_3)_3N\cdots SCO$	$(CH_3)_3N\cdots S\,{}^{13}CO$
r_{cm}/Å [b]	4.461(2)	4.429(2)	4.487(2)	4.470(2)
r(N···S)/Å [b]	3.063(2)	3.063(2)	3.061(2)	3.063(2)
k_σ/(N m^{-1}) [c]	7.60(3)	7.58(4)	7.43(3)	7.56(8)
)(10^{21} $k_{\theta\theta}$)/J [d]	4.808(1)	4.809(9)	3.405(1)	4.774(1)
$\langle\theta^2\rangle^{\frac{1}{2}}$/deg. [d]	12.686(1)	12.677(3)	12.795(1)	12.709(1)

[a] Absence of a mass number implies the most abundant nuclide.

[b] See eq.(2) and Figure 4 for definition. Errors are transmitted from assumed range of angles θ and ϕ. See text.

[c] The errors quoted for k_σ are those generated from the error is D_J and take no account of the fact that zero-point rather than equilibrium constants are used in eq.(5).

[d] The errors quoted for $k_{\theta\theta}$ and θ_{av} are those generated from the error in $2D_J + D_{JK}$ and take no account of the fact that zero-point rather than equilibrium constants are used in eqs.(6) and (7).

Table 4. Comparison of various properties[a] of the chalcogen-bonded complexes $(CH_3)_3N\cdots S{=}C{=}O$, $H_3N\cdots S{=}C{=}O$ and $H_3N\cdots S{=}C{=}S$

Complex	r(N···S)/Å	k_σ/(N m^{-1})	(10^{21}) $k_{\theta\theta}$ / J	θ_{av}/deg.	$\langle\theta^2\rangle^{1/2}$/deg.
$(CH_3)_3N\cdots SCO$ [b]	3.063(3)	7.60(3)	4.808(1)	12.0(6)	12.7(5)
$H_3N\cdots SCO$ [c]	3.3233(2)	4.687(9)	6.871	25.2	28.1
$H_3N\cdots SCS$ [d]	3.338(10)	3.95(2)	4.600(1)	27(3)	31.0(1)

[a] r(N···S), k_σ, $k_{\theta\theta}$, θ_{av} and $\langle\theta^2\rangle^{1/2}$ were determined by use of eqs. (2), (5), (6), (4) and (7), respectively.

[b] This work. [c] Ref. [26]. [d] Ref. [8].